ELSEVIER

Polymer 42 (2001) 7171–7180

polymer

www.elsevier.nl/locate/polymer

Poly(trimethylene teraphthalate) crystal structure and morphology in different length scales

Bojie Wang[a], Christopher Y. Li[a], Jennifer Hanzlicek[a], Stephen Z.D. Cheng[a,*], Phillip H. Geil[b], Janusz Grebowicz[c], Rong-Ming Ho[d]

[a]*The Maurice Morton Institute and Department of Polymer Science, The University of Akron, 170 University Circle, Akron, OH 44325-3909, USA*
[b]*Department of Materials Science and Engineering, University of Illinois, 1304 W. Green Street, Urbana, IL 61801, USA*
[c]*Shell Chemical Company, Westhollow Technology Center, Houston, TX 77251-1380, USA*
[d]*Department of Chemical Engineering, National Chung Hsing Univeristy, 250 Kuokuang Road, Taichung 402, Taiwan, ROC*

Received 5 September 2000; received in revised form 30 October 2000; accepted 15 November 2000

Abstract

Poly(trimethlene teraphthalate) (PTT) is one of the terephthalic polyester family members which can crystallize between its glass transition and melting temperatures. The crystal structure has been determined using both electron diffraction (ED) on single crystals and wide angle X-ray diffraction on powder and oriented fibers. The unit cell is triclinic with dimensions of $a = 0.46$ (3) nm, $b = 0.61$ (2) nm, $c = 1.86$ (1) nm, $\alpha = 97.5°$, $\beta = 92.1°$, and $\gamma = 110°$. The bulk PTT samples usually crystallize to form spherulites in the crystallization temperature (T_c) region studied. Between $T_c = 135$ and 165°C, the spherulites show a banded texture, and the band spacing increases with increasing T_c. The radial direction in the spherulites has been determined to be the crystal *a*-axis. Observations of successive ED patterns taken along the radial direction of a spherulite within one band reveal twist of lamellar crystals along the spherulite radial direction. The chain-folding direction, determined using a polyethylene decoration method, is along the *a*-axis direction in the lamellar crystals and parallel to the radial direction in the spherulites. Linear growth rates of the spherulites have also been measured and the maximum growth temperature is located at 165°C. This temperature is also the upper-limit temperature for PTT banded texture spherulite formation.

Keywords: Wide angle X-ray diffraction; poly(trimethylene teraphthalate); morphology

1. Introduction

Poly(trimethylene teraphthalate) (PTT) belongs to a series of engineering thermoplastic aromatic polyesters including poly(ethylene teraphthalate) (PET) and poly(butylene teraphthalate) (PBT). Although the synthesis of PTT using a polycondensation of terephthalic acid and 1,3-propanediol (trimethylene glycol) was reported as early as the 1950s, a recent new development in the synthesis of the monomer 1,3-propanediol using hydroformylation of ethylene oxide has been the key to launching a successful commercialization [1]. Mechanical performances of PTT are roughly between those of PET and PBT, and it can be melt-processed using a variety of processing methods to produce fibers, films and molded parts [2]. Of interest is that the mechanical properties of PTT are substantially enhanced, better than the PET and PBT counterparts, when the material is reinforced by glass or other high modulus short fibers [2].

The thermodynamic properties of PTT were recently reported [3]. This included heat capacities in both solid and liquid states, the amorphous glass transition temperature (T_g) at 37–42°C with a heat capacity increase at T_g of 94 J/(K mol), and the typical melting temperature in the region of 207–232°C. The equilibrium melting temperature (T_m^0) was assumed to be 237°C, and the heat of fusion (Δh_f^0) of 30 kJ/mol and the entropy of fusion of 58.8 J/(K mol) were calculated based on the measured heat capacity data. When PTT is crystallized, its T_g shifts towards higher temperatures, which can be as high as 58°C, depending upon crystallization conditions. This is typical of the behavior(s) of semi-crystalline polymers and has been widely observed in the past 20 years [4–6]. Rigid amorphous fractions in PTT were also identified and this fraction is less than that in PET and PBT [3].

Although crystal structures of other terephthalic polyesters such as PET and PBT have been widely studied,

* Corresponding author. Tel.: +1-330-972-6931; fax: +1-330-972-8626.
E-mail address: cheng@polymer.uakron.edu (S.Z.D. Cheng).

0032-3861/01/$ - see front matter
PII: S0032-3861(01)00046-5

only a few investigations on PTT have been reported [7–9]. The crystal structure of PTT was first determined using wide angle X-ray diffraction (WAXD) fiber patterns [7]. Unlike PBT [8,10–12], no structure transformation of PTT has been found after mechanical deformation, even though significant changes in unit cell dimensions were observed. A triclinic unit cell was reported with $a = 0.464$ nm, $b = 0.627$ nm, $c = 1.864$ nm, $\alpha = 98.4°$, $\beta = 93.0°$, and $\gamma = 111.1°$ [9]. Preliminary electron diffraction (ED) results in transmission electron microscopy (TEM) on solution grown PTT crystals were also reported, but only a single zone diffraction pattern which did not warrant a precise determination of unit cell lattice and symmetry [9]. These previously reported unit cell parameters of PTT crystal are still in debate because of the lack of detailed ED experimental analysis using stress-free crystals. Very recently, PTT crystal unit-cell parameters were determined using ED from both lamellar crystals and oligomers crystallized from the melt. Both reports found that the crystals are triclinic with parameters close to the previous report although with some deviations [13,14].

Banded spherulites are commonly observed in semicrystalline polymers. Generally speaking, lamellae in banded spherulites, specifically in polyethylene, are commonly considered to be twisting continuously along the radial direction due to the chain tilting in the lamellar crystals [15–22], although other opinions may also be found in literature [23–27]. A generalization of the detailed evolution of banded spherulites is still uncertain. Lamellar crystals serve as building blocks in constructing spherulites. Generally speaking, the growth of polymer lamellar crystals in the initial stage at lest, can be understood to divide into two catalogs. A lower rotational symmetric unit cell lattice should generate a more anisotropic habit of single crystals grown in the melt. For example, polyethylene (PE) in the orthorhombic form [28,29], isotactic polypropylene (i-PP) in the monoclinic α-form [30,31], syndiotactic polypropylene (s-PP) in the high-temperature orthorhombic form [32,33], poly(vinylidene fluoride) (PVDF) in the orthorhombic α-form and others, all show elongated [34,35], ribbon-like single lamellae. This implies that the growth rate along one unique axis is much faster than along any others. On the other hand, polymers such as PE in the high-pressure hexagonal form [36], isotactic polystyrene (i-PS) in the trigonal form [37,38], poly-4-methyl-1-pentene in the tetragonal form and others possess higher rotational symmetry in their crystal unit cells [39], and thus exhibit more symmetric polygonal lamellar habits [40]. These two types of single lamellar crystal precursors may undergo different pathways to form transient aggregates (hedrites/axialites) which evolve into the ubiquitous spherulites [41].

In this paper, we concentrate our study on the PTT crystal structure and morphologies in different length scales. The crystal structure is determined using both WAXD and ED in TEM experiments. Utilizing combined techniques of TEM, polarized light and atomic force microscopes (PLM and AFM), broad length scales of crystalline morphologies are covered. The key topics addressed here are the crystal structure in single lamellae, the banded structure in spherulites, the chain-folding direction in the crystals, the chain and crystal orientations in spherulites, and the linear crystal growth rates of PTT spherulites from the melt.

2. Experimental

2.1. Materials and sample preparations

The PTT material was kindly supplied by Shell Chemical Company at Westhollow Technology Center, Houston, TX. It was synthesized via polycondensation of terephthalic acid and 1,3-propanediol (trimethylene glycol). The intrinsic viscosity was 0.9 dl/g, measured in a 50/50 mixture of methylene chloride and trifluoroacetic at 30°C. The polymer was received in a powder form as-polymerized and thus without additives.

Samples for WAXD measurements were prepared by melting the PTT powder into films with a thickness of around 100 μm in order to obtain a good signal to noise ratio. The PTT fibers were first spun from the melt, further drawn until the complete necking was achieved, gradually heated to 150°C, and annealed free for one day before the measurements in order to obtain the maximum crystallinity. The fiber diameters were about 50 μm for the WAXD fiber experiments.

Polymer films with different thicknesses were also prepared for large-scale morphological observations using PLM experiments, and local scale morphological observations in TEM and AFM via spin-casting or solution casting from a concentration ranging from 0.05 (w/v)% to 5% solution using hexafluoropropanol as solvent. The thickness was controlled to be 50 nm for TEM and around 5 μm for PLM observation. The spherulitic formations and growth rates were monitored under PLM. The thin film samples prepared for TEM morphological observations were shadowed by Pt and coated with carbon. Mechanical shearing was also applied to PTT thin films in order to obtain orientated diffraction patterns using ED to compare with the results of WAXD fiber pattern. Solvent washing experiment was also carried out to investigate the inner part structure of PTT spherulite. Different ratio mixtures of hexafluoropropanol and chloroform were used as washing solvents.

2.2. Equipment and experiments

WAXD powder experiments were performed with a Rigaku 12 kW rotating anode generator (CuK_α radiation) equipped with a diffractometer. The film samples were mounted on aluminum sheets and the diffraction patterns were collected in reflection mode. Samples were scanned in a 2θ range between 1.5 and 35°. Background scattering was subtracted from the sample diffraction patterns. For isothermal crystallization, samples were that first heated

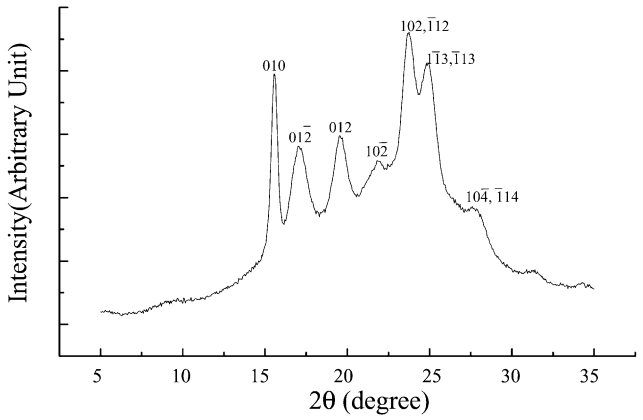

Fig. 1. WAXD powder pattern of PTT after the sample was crystallized at 150°C for 24 h. The diffraction peaks are assigned based on the unit cell structure determined from the WAXD fiber pattern shown in Fig. 2 and ED results shown in Fig. 4.

the samples to 20°C above their melting temperature ($T_m^0 = 237$°C), quenched to preset crystallization temperatures (T_c) and held there isothermally for various periods of time (several minutes to one day) for crystallization. After crystallization, samples were subsequently quenched in liquid nitrogen and brought to room temperature, which is below the PTT glass transition temperature ($T_g = 43$°C).

WAXD fiber patterns were obtained from a Rigaku Automated X-ray Imaging System (3000 × 3000 pixel resolution) with an 18 kW rotating anode X-ray generator. A 30 min exposure was required for a high quality WAXD fiber pattern. The background scattering was again subtracted from the fiber patterns. In order to determine the crystal structure and unit cell dimensions, computer refinements on the reflections of the fiber pattern were initially carried out using a program designed and written by us. The structural symmetry and unit cell dimensions were also checked based on the selective area ED (SAED) results (see below); a further refinement was conducted based on the reflections obtained from the WAXD powder pattern. This is because that the WAXD fiber patterns involved frozen stress caused by the high deformation ratios during the fiber spinning (see below).

Phase morphology was examined via a PLM (Olympus BH-2) and a Mettler hot stage (FP-90). The isothermal crystallization experiments were identical with those described previously. Linear crystal growth rates of PTT spherulites were measured at T_c in PLM. TEM experiments were carried out in a JEOL (1200 EX II) TEM using an accelerating voltage of 120 kV. Both bright field and dark field (BF and DF) images were obtained. SAED experiments were also conducted. ED calibration of the *d*-spacing was done using TlCl in a d-spacing range smaller than 0.384 nm, which is the largest spacing for TlCl. Spacing values larger than 0.384 nm were calibrated by doubling the d-spacing of those reflections based on their first order reflections. The replica method was also utilized to observe surface morphology of relatively thick film samples. Surface morphology was also examined using AFM (Digital Instruments Nanoscope IIIa) under ambient conditions. A 100 μm scanner was selected and tapping mode was used to obtain both height and phase images. The force used by the cantilever was light enough to limit damage to the sample, yet heavy enough so that the surface features could be accurately explored. The scanning rate was controlled to be 1–3 Hz for the low magnification images. The data was collected in 512 × 512 pixels per image.

3. Results and discussion

3.1. Crystal structure determination

Fig. 1 shows a PTT powder pattern at room temperature after the sample was heated to 250°C, held there for 2 min and then quenched to 150°C for isothermal crystallization for a duration of 24 h. Multiple reflections can be observed in this figure, indicating the formation of an ordered crystal structure. It should be noted that the sample used for obtaining this WAXD pattern does not introduce any external forces, such as uniaxial drawing as in the case of spinning PTT fibers. Therefore, this pattern may be used to generate stress-free unit cell dimensions if assignments of these reflections can be made based on the unit cell structures determined via WAXD fiber and ED patterns.

Generally speaking, the powder WAXD pattern is not sufficient to provide dimensionality of the crystal lattice since the number of reflections are limited, therefore an oriented specimen is desirable to determine crystal structure and unit cell dimensions. Fig. 2 is a PTT WAXD fiber pattern from a sample annealed at 150°C for 24 h. This fiber pattern is essentially identical to that previously reported. A total of eight reflections can be identified in Fig. 2. One reflection (010) is on the equator and one (002) on the meridian. In the quadrants, six reflections can be observed. Based on this WAXD fiber pattern, we can construct unit cell parameters of PTT using a reciprocal lattice. Preliminary results show that the crystals possess a triclinic structure. Their assignments are also included in this figure. The most obvious difference of PTT fiber patterns from those of PET or PBT is that, although all three materials possess triclinic unit cells, the meridian reflection does not obviously split in PTT fiber patterns while the (00*l*) reflections of PET and PBT are off-meridian. Previous publications indicate that there is about 1–2° split in this reflection spot; however, it is not obvious in either the literature or our results. ED patterns from mechanically sheared thin films should help solve this problem since ED pattern are taken within a local area where molecules may possess better orientation. Fig. 3 shows a sheared PTT thin film and the inserted SAED pattern with correct orientation. About a 2–3° tilt from the 'meridian' can be observed which is consistent with the triclinic unit cell.

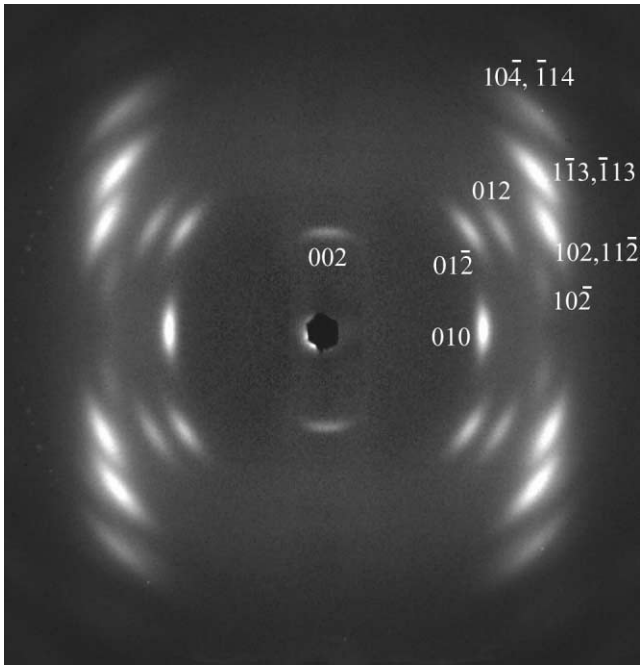

Fig. 2. WAXD fiber pattern of highly oriented PTT fibers after the sample was annealed at 150°C for 24 h.

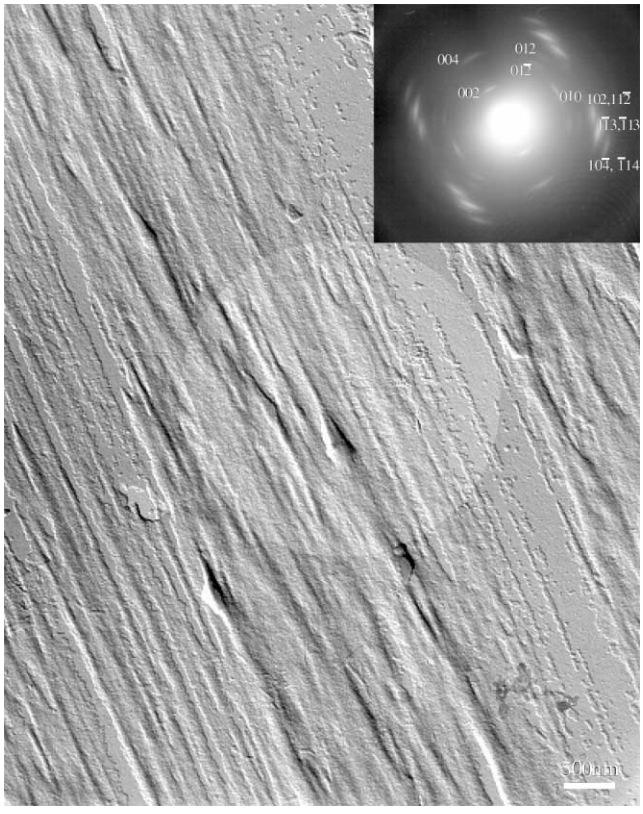

Fig. 3. TEM micrograph of PTT sheared thin film (a) and its corresponding ED pattern from the selected area (b) with the corrected orientation.

In order to examine quantitatively PTT crystals' reciprocal lattice, ED experiments on single crystals were conducted. The advantage is that the ED pattern directly provides a two-dimensional image of the reciprocal lattice of the single crystals and, by using tilting ED experiments, three-dimensional reciprocal space as well as crystal symmetry can be obtained. Fig. 4a–h shows a series of SAED patterns on a PTT single lamellar crystal with different zones obtained by tilting along the b^*-axis. Their assignments

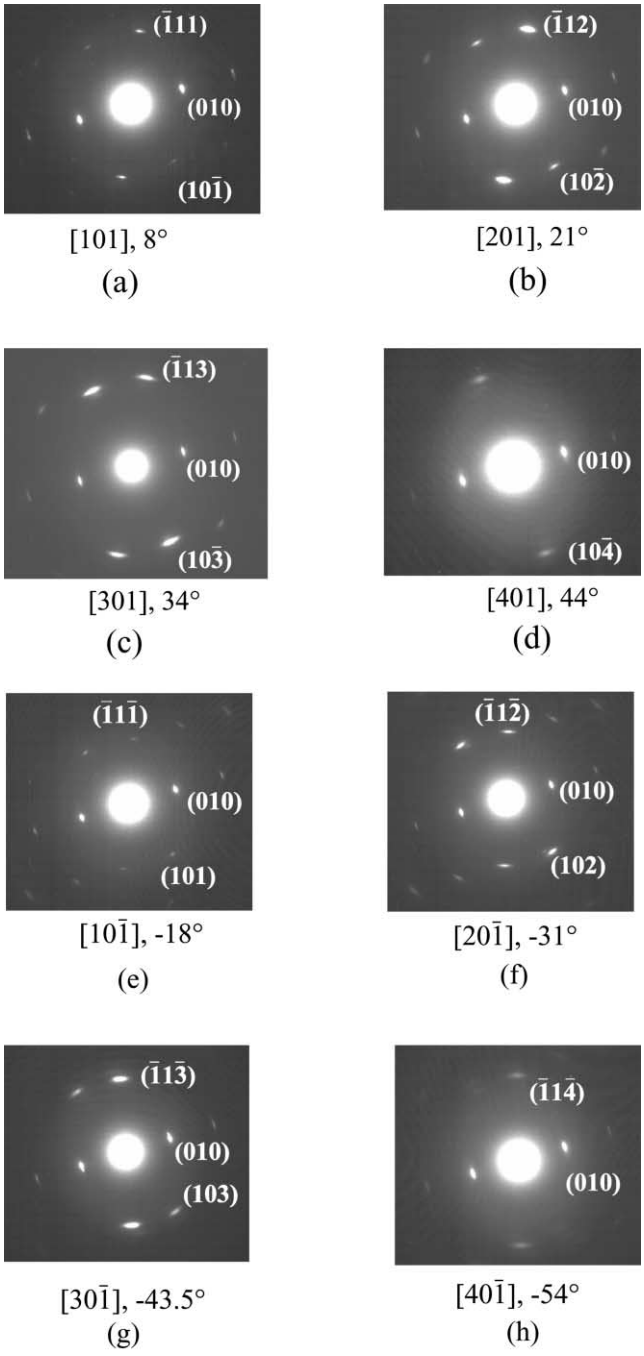

Fig. 4. Set of ED patterns with different zones of PTT crystals: the [101] (a), the [201] (b), the [301] (c), the [401] (d), the [10$\bar{1}$] (e), the [20$\bar{1}$] (f), the [30$\bar{1}$] (g), and the [40$\bar{1}$] (h).

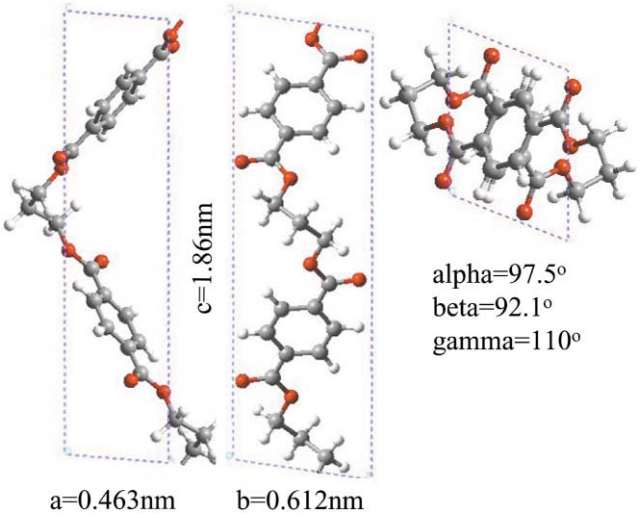

Fig. 5. Atomic positions of PTT chains in the crystal unit cell.

are also included in these figures based on the triclinic lattice. These ED patterns consist of the [101], [201], [301], [401] and [10$\bar{1}$], [20$\bar{1}$], [30$\bar{1}$], [40$\bar{1}$] zones, respectively and provide the crystal symmetry of $P1$ of the triclinic unit cell. Based on this structure, the reflection peaks in the WAXD powder pattern (Fig. 1) can also be assigned. Further refinement using the d-spacing data obtained from the WAXD powder pattern in Fig. 1 shows that the crystal structure is triclinic with dimensions $a = 0.46$ (3) nm, $b = 0.61$ (2) nm, $c = 1.86$ (1) nm, $\alpha = 97.5°$, $\beta = 92.1°$, and $\gamma = 110°$. The crystallographic density is 1.40 g/cm^3.

Of interest is that the (100), (110) reflections are intrinsically weak. Computer calculation of the chain packing in this triclinic unit cell shows that indeed, the intensity of the (100) plane is only 1% of the (010) plane. The detailed atomic positions in the unit cell are shown in Fig. 5. This must be because the structure factors of these crystalline planes are small, which should be related to the arrangement of polymer chains in the crystal. The ratio between the unit cell c-axis dimension and the extended chain length is only about 75%, indicating a big zigzag chain conformation along the c-axis. It should be noticed that in the cases of PET and PBT, this ratio is as high as 97 and 92%, respectively. PTT molecules are therefore easier to be deformed in the crystals when the sample is drawn compared with PET and PBT, which also answers why large deviations of the unit cell dimensions of PTT have been reported, although no structural transformation has been observed during drawing.

3.2. Banded structure, chain and crystal orientations in spherulites

Generally speaking, PTT bulk samples form spherulites when crystallized from the melt. Fig. 6a–h shows a series of PLM observations of spherulitic textures formed at different isothermal crystallization temperatures (T_cs). The Maltese cross can be clearly seen in these figures. These spherulites

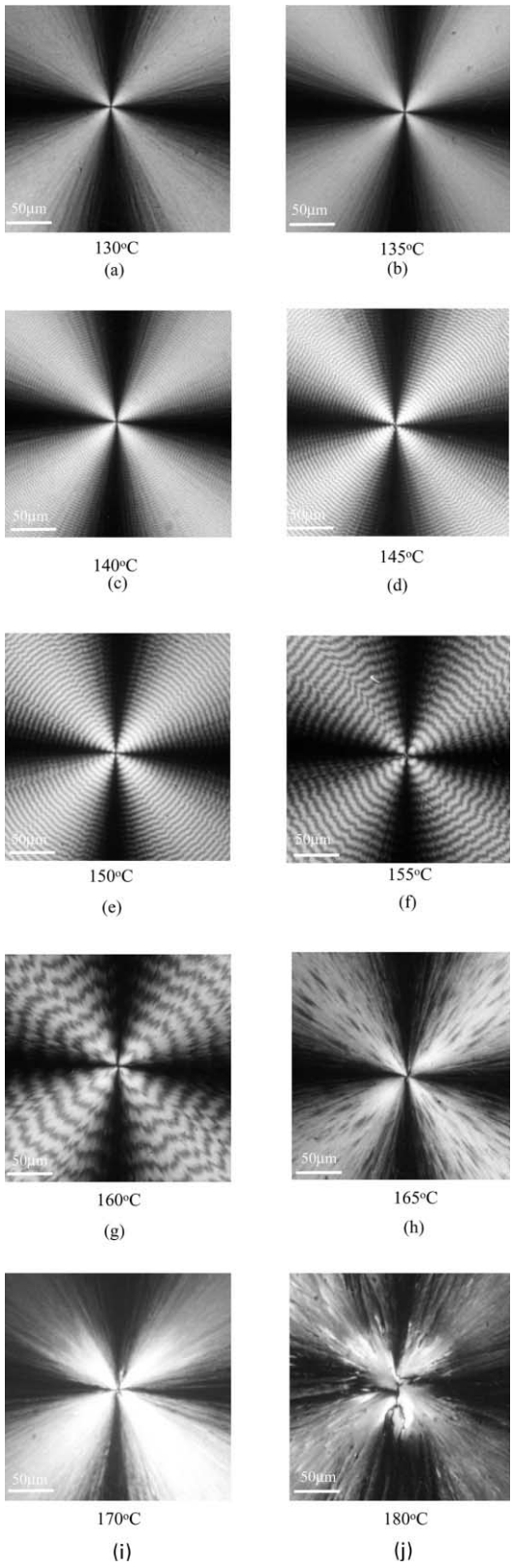

Fig. 6. Set of PLM microphotographs of spherulites of PTT crystallized at 130°C (a), 135°C (b), 140°C (c), 145°C (d), 150°C (e), 155°C (f), 160°C (g), and 165°C (h). The banded texture starts at 135°C and disappears at 165°C.

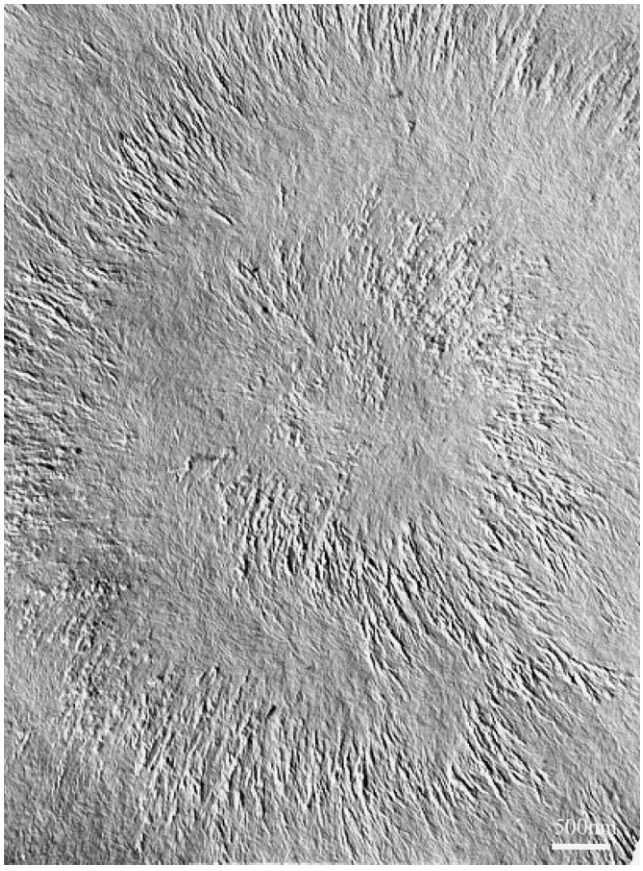

Fig. 7. Banded structures of PTT spherulites observed using replica method in TEM.

can be identified as having negative birefringence by inserting a Gypsum plate into the light path. In addition, when T_c is between 135 and 165°C, banding can be found in the spherulites. The spacing of bands increases with increasing T_c. For example, at $T_c = 135$°C the band spacing is 1 μm, and it increases to 4 μm when $T_c = 165$°C. It was also found that the band spacing is dependent upon the sample thickness, thinner samples form smaller band spacing. Details of the banded structures can be examined in TEM using replicas, as shown in Fig. 7, and AFM in Fig. 8a–c. In addition to clearly observing the banded structures in these spherulites, the organization of these bands is particularly interesting; this is shown most clearly in AFM results. For the normal case, as shown in Fig. 8a, the bands possess the same origin (the primary nucleation site) and form closed circles with quantized radius of *nd*, where *n* is an integer number and *d* is the spacing of the neighboring bands. However, in Fig. 8b, one can see that spiral-type of bands initiated from the primary nucleation site. A possible reason is that it may due to a non-diametral section of a three-dimensional spherulite. In Fig. 8c, the bands show a sudden shift (marked by an arrow) along a radial line from the primary nucleation site. A clear boundary of this shift can be seen. This sudden shift may be viewed as a defect of bands during the spherulitic radial growth in the length scale of micrometers. The formation mechanism is under investigation.

In order to understand the chain orientation in these banded structures and the crystal orientations in the spherulites, we have carried out ED experiments along the radial direction of one spherulite within one band distance. The key problem is to prepare spherulites within a certain thickness range: thin enough for electron beams to pass through while thick enough to ensure the formation of banded textures, since it is extremely difficult to recognize the banded textures for a very thin sample (thinner than ~50–100 nm). Fig. 9 shows the ED results. Within one band distance, three ED patterns were obtained. Detailed analysis shows that these three patterns can be assigned as the $[12\bar{1}]$, $[24\bar{1}]$, and $[00l]$ zones, respectively. The spherulite radial direction can thus be determined to be the crystal *a*-axis, and these three diffraction patterns also demonstrate that lamellae indeed twist along this radial direction since the $[12\bar{1}]$ and $[24\bar{1}]$ zones can be obtained by tilting the $[00l]$ zone ED along the crystal *a*-axis. One can calculate the angles between two neighboring zones; they are ~30° between the $[12\bar{1}]$ and $[24\bar{1}]$, and ~60° between the $[24\bar{1}]$ and $[00l]$, respectively. Since the neighboring bands represent a 180° twisting of the lamellae, we should observe as many zones as we did in the single lamellae ED tilting experiments as shown in Fig. 4. The absence of other possible zone diffractions indicates that the lamellar twisting in the spherulites may follow certain preferred orientations. Fig. 10, which is a TEM micrograph of a replica of PTT banded spherulites, shows that the edges of lamellae possess certain orientations. However, it again may be due to a non-diametral cross-section of a three-dimensional spherulite.

As discussed before, banded texture becomes more difficult to observe as the film becomes thinner than ~50–100 nm. However, a solvent washing experiment on a thick sample (thickness of about 0.5 μm) can explore banded textures on an otherwise more or less featureless spherulite. Fig. 11a is a film surface morphology before washing and Fig. 11b is the same sample after washing. After the washing experiments, the film thickness decreases to around 100 nm. It is evident that the solvent washed out almost all of the relatively flat-on lamellae of the spherulites while some of the edge-on lamellae remain. It may be understood that amorphous parts of the spherulite are easier to be dissolved comparing with the crystalline lamellae. For flat-on lamellae in the spherulite, the amorphous crystal surfaces are exposed to the solvent, and thus can relatively easily be washed off if, while for the edge-on crystals, the solvent must penetrate between the crystals to reach the amorphous surface of the lamellar crystals. This experiment again proves the different orientations of lamellae within the banded spherulite. By controlling the ratio of hexafluoropropanol and chloroform and washing time, the inner part of thick spherulites can be observed as shown in Fig. 12, lamellar crystals within one band seems to have certain preferred orientations as discussed in the section of TEM replica

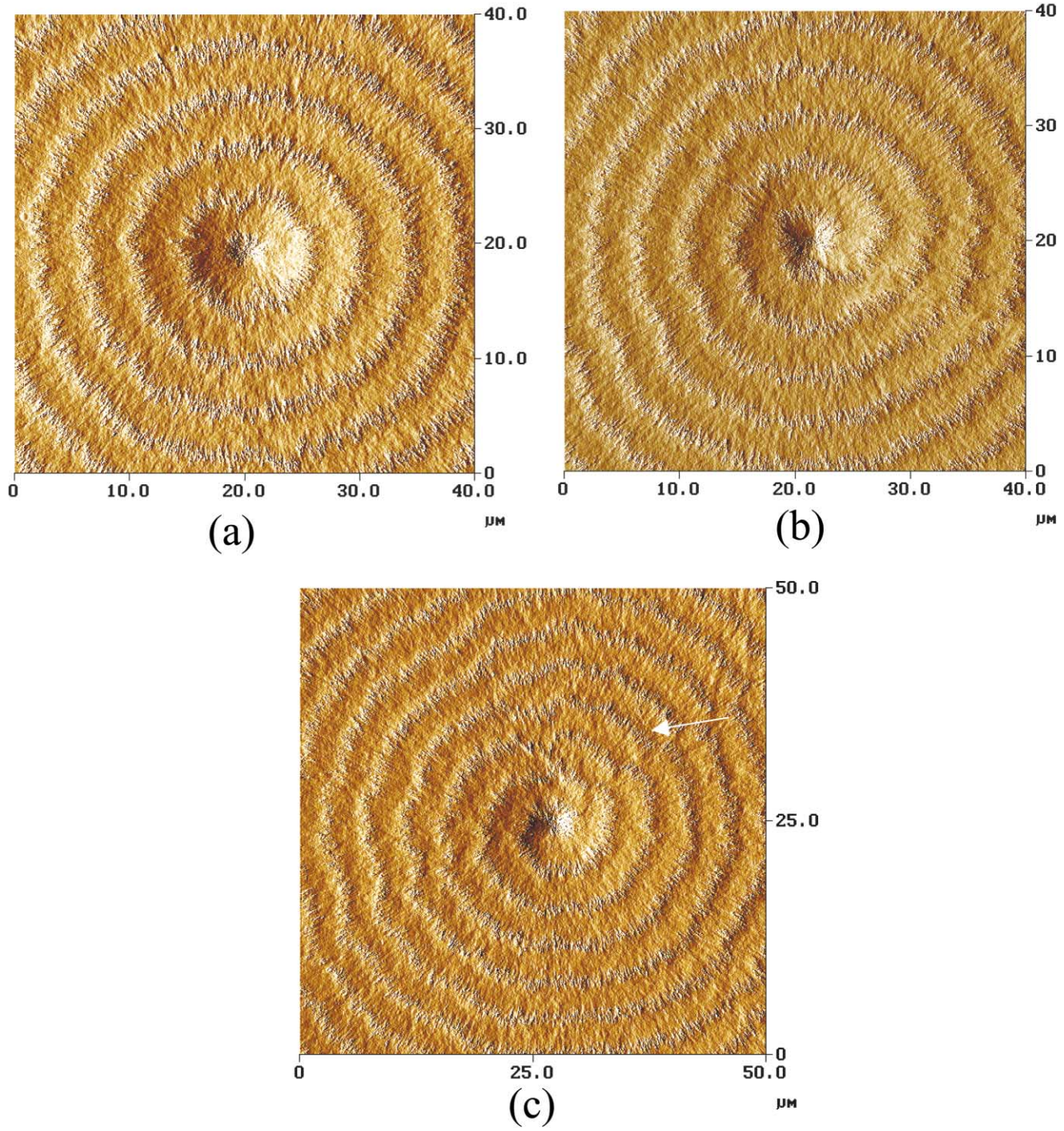

Fig. 8. Banded structures of PTT spherulites observed in AFM: a regular banded spherulite (a); a spherulite with a band started at the primary nucleation site (b); and a spherulite with band defects along the radial direction (marked by an arrow) (c).

experiment. Further investigation is necessary to provide more detailed explanations.

DF experiments on PTT spherulites, using both the (010) and (012) diffractions, show alternating bright and dark bands (Fig. 13). The bright bands are the areas giving rise to the (010) and (012) diffractions, and the dark bands represent the areas where the crystals do not contribute to these two diffraction spots due to their orientation. This again proves that the lamellar crystals in PTT spherulites are twisting. Of interest is that DF images using the (010) and (012) gave bright bands with a width about 2 μm, which is much more than expected. This could be caused by lamellae cooperatively twist to form a continuous edge shift of neighboring lamellae during its growth, or due to certain preferred orientations of the lamellae. Since our DF experiments were conducted using thin film samples, this preferred orientation

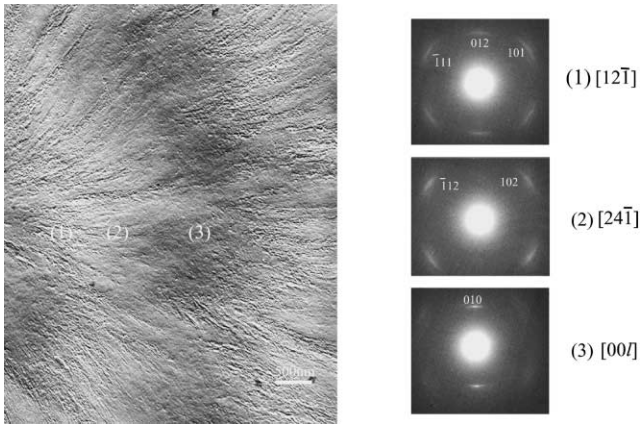

Fig. 9. Set of SAED patterns along the radius direction of spherulitic growth within one band: the [12$\bar{1}$] zone (a); the [24$\bar{1}$] zone (b); and the [00l] zone (c). The circles in the TEM morphological micrograph are the locations where these SAED patterns were taken.

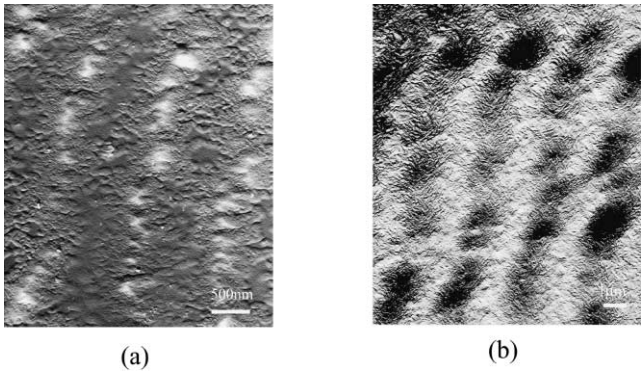

Fig. 11. TEM micrograph of PTT thick film morphology using the replica method; band texture can be hardly seen (a), TEM micrograph of the PTT film after solvent washing using 4:1 chloroform: hexofluoropropanol. Flat-on lamellae of the spherulites have been washed away and most of the edge-on lamellae crystals still remain. Banded texture can thus be clearly seen (b).

of the lamellae could possibly be caused by the surface confinement. More detailed investigations are necessary to fully reveal the mechanism of lamellar twisting in PTT spherulites.

3.3. Chain folding and linear crystal growth rates

The chain folding direction can be studied via the PE decoration method [42,43]. In most of the cases, this method has been used for lamellar single crystals. We tried to use it on PTT spherulites. Fig. 14a and b shows PE decorated PTT spherulites, in which Fig. 14a is within one spherulite and Fig. 14b is near a boundary of two spherulites which are impinged with each other. It is clear that the needle-like PE crystals are more or less perpendicular to the radial growth direction of the spherulites. Since the *c*-axis of the PE crystals is normal to the needle direction, the chain folding of PTT crystals has to be parallel to the radial growth direction, namely, along the crystal *a*-axis. Of interest is that the chain folding is not along the surface of the growth front as commonly described, but is towards the melt. This has also been found in some other polymers [44,45]. One of the possibilities is that the growth

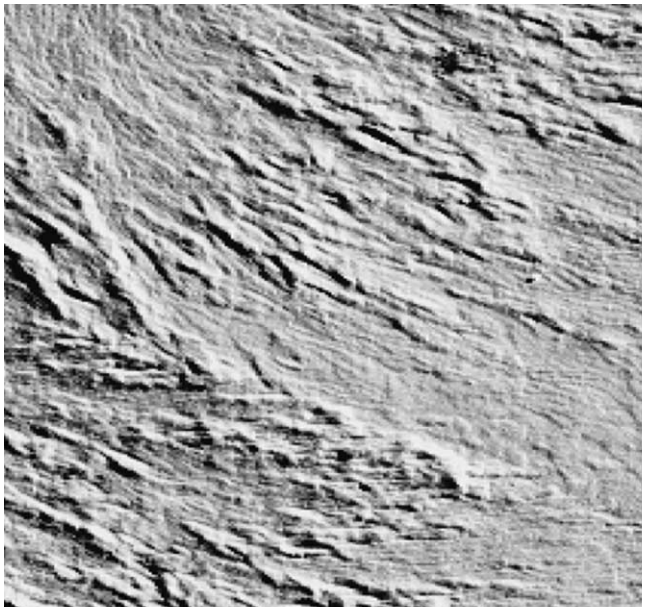

Fig. 10. TEM replica of PTT band texture showing the certain orientation of lamellae within each band distance.

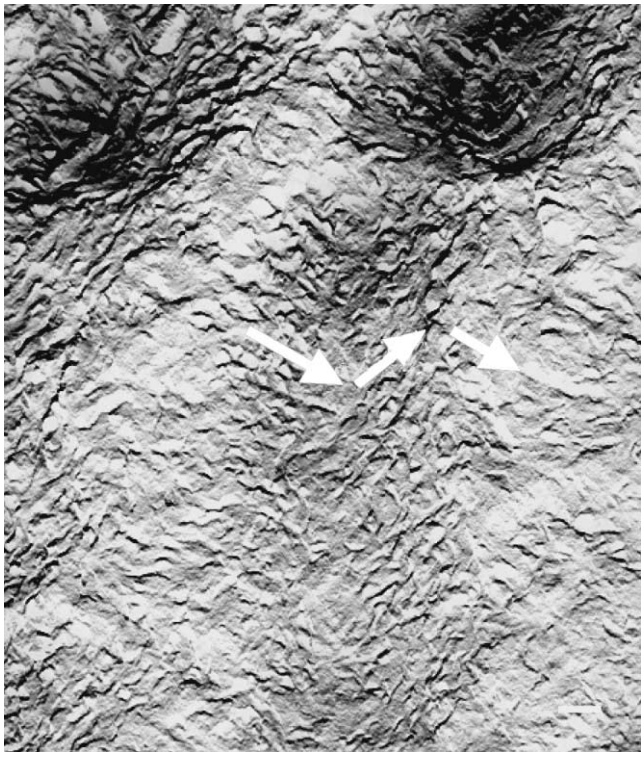

Fig. 12. TEM micrograph of PTT spherulite after solvent washing of a relatively thick film. The same mixed solvent was used. Lamellar orientation changes can be seen.

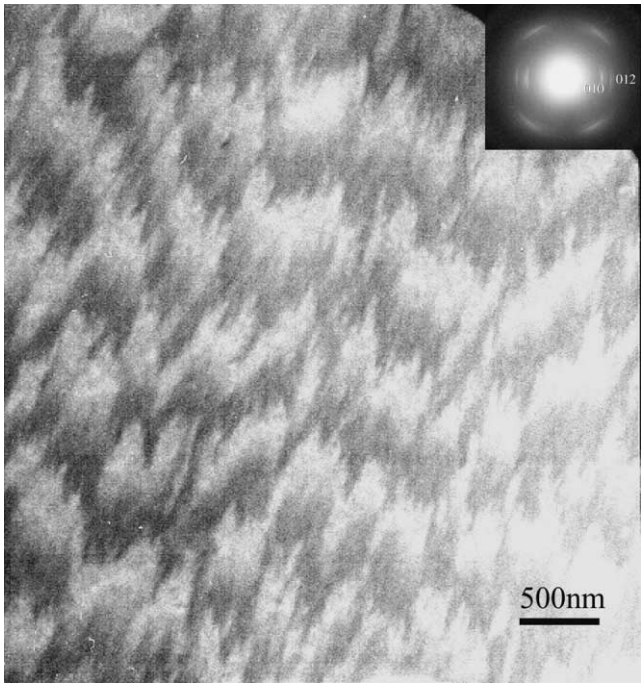

Fig. 13. The (010) and (012) dark field image of a PTT spherulite.

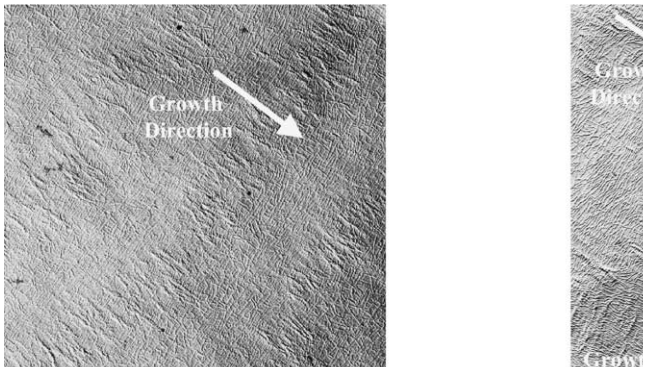

Fig. 14. Set of surface replica TEM micro-graphs of a PE decorated spherulite (a), and spherulites where impingement occurs (b).

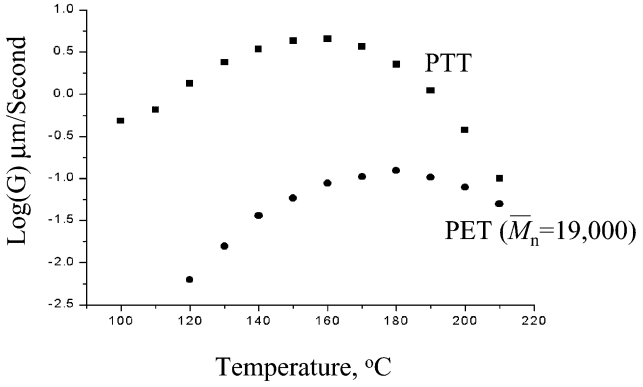

Fig. 15. PTT linear spherulitic growth rates changes with T_c. A growth rate maximum at 165°C is clearly shown.

front is rough and tooth-like. In this case, the lateral surface free energy is smaller than the fold surface energy and crystal growth rates are basically determined by the folded surface free energy based on the nucleation theory.

Fig. 15 shows linear crystal growth rates of the spherulites at different T_cs between 100 and 200°C. The linear growth rate data of PET obtained by van Antwerpen et al. are also included for comparison [46]. It is clear that PTT crystal growth rates are generally much faster than the corresponding PET at the same undercooling. The maximum growth rate for PTT appears at 165°C and the growth rate curve exhibits a bell-shape, namely, when T_c increases to approach the T_m or decreases to approach T_g, the growth rate decreases. Furthermore, it is interesting to find that the T_c at which the maximum growth rate is observed is coincident with the disappearing of the banded structure in spherulites. This indicates that the banded structure can only be formed in the lower half of the bell-shaped curve down to the T_g.

4. Conclusions

The crystal structure of PTT has been determined. It is triclinic, space group $P1$, with $a = 4.58$ nm, $b = 0.6.1$ nm, $c = 1.86$ nm, $\alpha = 97.5°$, $\beta = 92.1°$, $\gamma = 110°$. PTT crystallizes into spherulites. Between $T_c = 135$ and 165°C, banded spherulites form. Above 165°C, the band structure disappears. This temperature also corresponds to the maximum spherulite crystal growth rate. Banded spherulites are caused by lamellar twisting along the a-axis, which is parallel to the radius direction of the spherulite growth. It is surprising to find that the chain-folding direction is parallel to this radius direction. This may imply that the chain molecules fold into the melt during the crystal growth.

Acknowledgements

This work was supported by the NSF (DMR-9617030).

References

[1] Traub HL. Die Angew Makromol Chem 1995;179:4055.
[2] Dangayach K, Chuah H, Gergen W, Dalton P, Smith F. 1997 ANTEC Conference Shell Chemical Company.
[3] Pyda M, Boller A, Grebowicz J, Chuah H, Lebedev BV, Wunderlich B. J Poly Sci Part B: Poly Phys 1998;36:2499.
[4] Cheng SZD, Wunderlich B. Macromolecules 1986;19:1868.
[5] Cheng SZD, Pan R, Bu SH, Cao MY, Wunderlich B. Makromol Chem 1988;189:1579.
[6] Cheng SZD, Wunderlich B. J Poly Sci Part B, Polym Phys 1986;24:1755.
[7] Goodman I. Angew Chem 1962;74:606.
[8] Jakeways R, Ward IMIM, Wilding MA, Hall IH, Desborough IJ, Pass MG. J Polym Sci Polym Phys Ed 1975;13:799.
[9] Poulin-Dandurand S, Perez S, Revol JF, Brisse F. Polymer 1979;20:419.

[10] Yokouchi M, Sakakibara Y, Vhatani Y, Tadokoro H, Tanaka T, Yado K. Macromolecules 1976;9:266.
[11] Liu J, Geil PH. J Macromol Sci Phys 1997;36:263.
[12] Hall IH, Pass MG. Polymer 1976;17:807.
[13] Ho RM, Ke KZ, Chen M. Macromolecules 2000;33:7529.
[14] Yang J, Sidoti G, Liu J, Geil PH. Polymer 2001;42(15).
[15] Keller A. J Polym Sci 1955;17:351.
[16] Keith HD, Padden Jr. FJ. J Polym Sci 1959;39:101.
[17] Keith HD, Padden Jr. FJ. J Polym Sci 1959;39:123.
[18] Price FP. J Polym Sci 1959;39:139.
[19] Keller A. J Polym Sci 1955;17:151.
[20] Fujiwara Y. J Appl Polym Sci 1960;10:271.
[21] Keith HD, Padden Jr. FJ. Polymer 1984;25:28.
[22] Keller A. J Polym Sci 1955;17:291.
[23] Bassett DC, Hodge AM. Polymer 1978;19:649.
[24] Bassett DC, Hodge AM. Proc R Soc 1978;A359:121.
[25] Bassett DC, Hodge AM. Proc R Soc 1981;A377:25.
[26] Bassett DC, Hodge AM. Proc R Soc 1981;A377:39.
[27] Bassett DC, Hodge AM. Proc R Soc 1981;A377:61.
[28] Toda A. Colloid Polym 1992;270:667.
[29] Toda A, Keller A. Colloid Polym 1993;271:328.
[30] Sauer JA, Morrow DR, Richardson GC. J Appl Phys 1965;36:3017.
[31] Lotz B, Graff S, Straupe C, Wittmann JC. Polymer 1991;32:2902.
[32] Lotz B, Lovinger AJ, Cais RE. Macromolecules 1988;21:2375 (and a series of publications followed in Macromolecules).
[33] Bu Z, Yoon Y, Ho RM, Zhou W, Jangchud I, Eby RK, Cheng SZD, Hsieh ET, Johnson TW, Geerts RG, Palackal SJ, Hawley GR, Welch MB. Macromolecules 1996;29:6575.
[34] Briber RM, Khoury FA. J Polym Sci Polym Phys Ed 1993;31:1253.
[35] Toda A, Arita T, Hikosaka M. Polymer, 2001;42:2223.
[36] DiCorleto JA, Bassett DC. Polymer 1990;31:1971.
[37] Keith HD. J Polym Sci Part A 1964;2:4339.
[38] Keith HD, Padden Jr. FJ. J Polym Sci Polym Phys Ed 1987;25:2371.
[39] Patel D, Bassett DC. Proc R Soc Lond A 1994;445:577.
[40] Keith HD, Padden Jr. FJ. Polymer 1986;27:1463.
[41] Khoury F. Private communication.
[42] Wittmann JC, Lotz B. Makromol Rapid Commun 1982;3:733.
[43] Wittmann JC, Lotz B. J Polym Sci, Polym Phys Ed 1985;23:205.
[44] Lovinger AJ. J Appl Phys 1978;49:5014.
[45] Jones NA, Atkins EDT, Hill MJ, Cooper SJ, Franco L. Polymer 1997;38:2690.
[46] Van Antwerpen F, Van Antwerpen DW. J Polym Sci Polym Phys Ed 1972;10:2423.